

**PROCESSING OF POROUS ALUMINA
CERAMICS USING NATURAL FOAMING
AGENT**

A THESIS SUBMITTED IN PARTIAL FULFILMENT OF

THE REQUIREMENT FOR

**MASTER OF TECHNOLOGY (DUAL DEGREE)
IN**

INDUSTRIAL CERAMICS

By

Abhijeet Sarangi

710 CR 1180

Under the guidance

of

Prof. Santanu Bhattacharyya



Department of Ceramic Engineering

National Institute of Technology, Rourkela

2015



DEPARTMENT OF CERAMIC ENGINEERING

National Institute of Technology,

Rourkela-769008

CERTIFICATE

This is to certify that the thesis entitled, “PROCESSING OF POROUS CERAMICS USING NATURAL FOAMING AGENT” Submitted by ABHIJEET SARANGI (710 CR 1180) in partial fulfillment of the requirement for the award of MASTER OF TECHNOLOGY (DUAL DEGREE) IN INDUSTRIAL CERAMICS at the NATIONAL INSTITUTE OF TECHNOLOGY, ROURKELA is an original work carried out by him under my supervision and guidance. To the best of my knowledge, the contents exemplified in the thesis have not been submitted to any other University/Institute for the award of any Degree or Diploma.

Date:

S.BHATTACHARYYA

ACKNOWLEDGMENT

I wish to express my sincere thanks to **Prof. Santanu Bhattacharyya**, Department of Ceramic Engineering, N.I.T. Rourkela, for allocating me the project “Processing of Porous Ceramics Using Natural Foaming agent”. His guidance and the suggestions he offered has helped me all through this project work.

I would like to express my appreciation to all the faculty members for their collaboration amid this project work. My genuine thanks to the Research Scholars, M. Tech students and the non-teaching staff for their assistance.

Last but not least, my solemn thanks to all my friends who have who have calmly augmented a wide range of support for accomplishing this endeavour.

Abhijeet Sarangi

M.Tech (Dual Degree)

Ceramic Engineering

LIST OF FIGURES

Figure No.	Figure Caption	Page No.
1.	Schematic diagram of Porous ceramics prepared by the of Removal of Fugitives	15
2.	Schematics of Replica processing method.	17
3.	Schematics of Direct foaming process method.	19
4.	Time schedule for sintering of samples at 1500° C	22
5.	Flow chart related to slurry preparation (a) Stirring method (b) Tumbling method	23
6.	Standard curve for determination of Amphipathic Glycoside obtained using UV Visible Spectrophotometer	27
7.	Particle size distribution of calcined alumina	29
8.	Viscosity at different Darvan C concentration	29
9.	Rheological behaviour of alumina slurry with binder	30
10.	Photographs of samples with Sucrose as binder and AG	31
11.	Photograph of trial sample prepared with 35 vol. % solid loading, 5 % PVA, 0.1 % Pore former and 0.3 % Darvan C	32
12.	Photograph of surface of the samples dried at (a) 50°C (b) 60°C (c) 70°C and (d)80°C	33
13.	Samples Prepared by Stirring method	34
14.	Samples Prepared by Tumbling method	35
15.	Optical Microscope Microstructure of (a) 35 vol % solid loading, PVA 5 %, pore former 3 % by stirring method (b) 35 vol % solid loading, PVA 5 %, pore former 3 % in tumbling method.	37
16.	Optical microstructural images of (a) 30 vol. % with 1.5 % pore former, (b) 30 vol. % with 3 % pore former (c) 30 vol. % with 4.5 % pore former	39
17.	Effect of Binder content on particle separation in green tape from “Principles of ceramic processing” [5], 40, (1974) J. Reed.	39
18.	(a) 25 vol. % with 5 % PVA, (b) 30 vol. % with 5 % PVA (c) 35 vol. % with 5% PVA (d) Microstructure of sample made from 35 vol. % solid loading, 3 % pore former and 5% PVA showing interconnection between pores	40
19.	FESEM microstructure of (a) 30 vol. % alumina, 1.5 % pore former, 5 % PVA (b) 35 vol. % alumina, 1.5 % pore former, 5 % PVA(a) 30 vol. % alumina, 3 % pore former, 5 % PVA (a) 35 vol. % alumina, 3 % pore former, 5 % PVA	41

LIST OF TABLES

Table No.	Table Caption	Page No.
1	Drainage rate of liquid with various binder [Mahua (Madhuca Longifolia), Guar Gum, Sucrose, PVA], varying their intensity with AG.	28
2	Summary of Apparent porosity, Total Porosity, Closed porosity, Bulk Density and CCS of the samples prepared with different concentration of PVA as Binder and Amphipathic Glycoside concentration.	40

ABSTRACT

The aim of this work was to fabricate Porous Alumina ceramics direct foaming method using Amphipathic Glycoside as the foaming agent and a pore former. The porosity in the porous body was dependent on the foam stability, Nature of the binder, Al_2O_3 amount in the slurry and slurry preparation method. Thus, processing parameters like drying temperature, slurry preparation process, binder concentration, pore former concentration and solid loading was optimized. This optimized composition resulted in the fabrication of a porous body after sintering. To further stabilize the foam and to get an interconnected porous body Glycerol was added to increase the foam stability and particle attachment to the foam. In this study, it is found that with a rise in pore former concentration, apparent porosity decreased. But with an increase in solid loading apparent porosity increases due to particle attachment to the foam. When we added glycerol to the slurry along with a change in slurry preparation method, interconnectivity between pores increased.

CONTENTS

Certificate

Acknowledgements

List of figures

List of tables

Abstract

Chapter – 1 Introduction

1.1. Classification of porous ceramics 11-12

Chapter – 2 Literature Review 14-20

Chapter – 3 Experimental details

3.1. Preparation of Amphiphatic Glycoside Extract 21

3.1.1.. Determination of Glycoside Concentration 21

3.2. Foam stability with different binders 21

3.3. Optimization of Deflocculant concentration 21

3.4. Rheological Study of the slurry 21

3.5. Slurry preparation 22

3.6. Casting and Drying 22

3.7. Sintering 22

3.8. Characterizations

3.8.1. Apparent Porosity and Bulk Density 25

3.8.2. Total Porosity and closed porosity 25

3.8.3. Optical Microscope Microstructure 25

3.8.4. Measurement of compressive strength	26
3.8.5. FESEM Microstructure	26
Chapter – 4 Results and Discussions	
4.1. Determination of concentration of Glycoside in the pore former extract	28
4.2. Comparison of liquid drainage with different binders	28
4.3. Particle size analysis of Calcined Alumina	30
4.4. Optimization of the deflocculant concentration	30
4.5. Rheological analysis of alumina slurry	31
4.6. Samples prepared with Sucrose as binder and AG	32
4.7. Samples made with PVA as binder and AG	
4.7.1. Trial sample prepared with PVA as binder and AG as pore former	33
4.7.2. Optimization of the drying temperature	33
4.7.3. Alumina Slurry preparation by tumbling method	35
4.7.4. Effect of slurry preparation process on the nature of porous sample formed	36
4.8. Effect of glycerol on the microstructure development in porous alumina	38
4.8.1. Variation of porosity and strength with pore former concentration	38
4.8.2. Variation of porosity and strength with solid loading and pore former concentration	39
4.8.3. Variation of microstructure with change in pore former concentration and solid loading	42
Chapter – 5 Conclusion and scope of further work	44-45
References	

CHAPTER 1

INTRODUCTION

INTRODUCTION

Porous ceramic materials with porosity in the range of 20-97% are becoming an important member of ceramic materials owing to their fascinating functional and structural properties under different service conditions. ^[1] Some of the key features of porous ceramics are open pore structure, low thermal conductivity and tailored pore size distribution. Recently, active cooling has become the most efficient mode of cooling of panels in the spaceflight to prevent high thermal shock. The dynamic cooling process uses a coolant that is infiltrated or injected into a porous ceramic and is later given out for thermal protection by reducing the bulk temperature. ^[2] It is used in supports for catalysts, piezoelectric ceramics, bone scaffolds, ceramic filters and electrodes in fuel cells. ^[3]

Porosity in ceramics is created through some methods. The natural and easiest of them are to terminate the sintering or densification of the fabricated body prematurely so that residual pores remain in the sintered body. This method is known as partial sintering method. ^[1] All the other methods include incorporation of fugitives, which may be solid, liquid or gas. Among the solid fugitives Naphthalene ^[4], corn starch ^[5], cotton ^[6] are the prominent ones. In the liquid fugitive systems, water, liquid paraffin, salicylic acid are the more important variety. ^[7] Use of porous template for creating a positive or negative replica followed by removal of the template is another versatile method of fabricating porous body. ^[8-11] In the direct foaming method, foams are generated in the slurry by the agitation of a foaming agent and the ceramic material ^[12, 13]. In the Gel Casting method, the gelling of ceramic suspension is achieved through a chemical reaction between long chain organic materials such as MAM (methyl-acrylamide) and MBAM (methylene-bis-acrylamide).^[14, 15] Some other additives achieve gelation through their hydrolysed species; examples are the use of corn starch ^[16], guar gum ^[17], sunflower oil ^[18] etc. Subsequent firing operation removes the

additives leaving behind a porous body. In another technique, foams are generated by adding foaming agents like egg white ^[19], saponin ^[20], etc. which creates foam on stirring. The stability of the foam decides the pore size and porosity in the samples. ^[21, 22] There are also some other non-conventional techniques like freeze casting ^[23, 24], rapid prototyping ^[25], etc. which have also been successfully used to create porous ceramics.

1.1. Classification of porous ceramics

Depending on the pore diameter, the porous materials are classified into three classes. Macro-porous ($d > 50$ nm), meso-porous ($50 \text{ nm} > d > 2$ nm) and micro-porous ($d < 2$ nm) ^[26]. On the basis of the fabrication process, porous ceramics can have either open or closed pores or a combination of both. Open pores are open at the surface, and closed pores are isolated pores sealed from the surface. ^[21]

Porous ceramic products can also be categorized according to the inner structure (granular, cellular, fibrous). On the basis of the end use or application area, they can be classified as heat insulating (main parameter: thermal conductivity), heat shielding (main parameter: product of thermal conductivity and apparent density values) and permeability (main parameters: porosity, pore size and permeability). ^[27] Depending on the pore interconnectivity, cellular ceramics can be divided into two categories: (a) Reticulate ceramics and (b) Foam ceramics. Reticulate ceramics has interconnected pore structure that are surrounded by a web of ceramic struts. A polymeric sponge pre-form is infiltrated by a ceramic suspension that is then dried and sintered. The process leads to an open porous ceramic structure, characterized by a hollow strut due to burning out of the preform. ^[28] Direct foaming method is used in the fabrication of foam ceramics in which gas is directly incorporated into the liquid medium by mechanical agitation. The total porosity in foam ceramics depends on the amount of incorporated or injected gas that in the liquid medium

during the foaming process. The pores generated can be either open or closed depending on the wet foam processing. Pores with window structure are obtained if the accumulation of particles takes place at the junction of foam wall due to bubble disproportionation. But the closed pores are formed when particles get uniformly distributed around the gas bubbles and settle upon drying. ^[1]

In the summary, it can be said that porous ceramics is an important class of ceramics having diversified applications ranging from catalysts, filters, heat insulating materials, etc. However depending on the exact application area, the fabrication routes will vary to produce either a foamed ceramics or a reticular ceramics or a combination of both. Depending on the processing method, the type of pore-forming agent and the solid loading, foams will produce either an isolated porous ceramics or an interconnected porous body. This thesis will aim to provide a wide variety of porous ceramics using a natural pore former.

CHAPTER 2

LITERATURE REVIEW

LITERATURE REVIEW

Porous ceramics is used in severe conditions that include the highly corrosive environment. Some of its applications include filtration of hot molten metals, support in catalytic reactions, thermal insulation at high temperature, filtration of gasses from diesel engine exhaust, etc. For such applications, the material should have high surface area, thermal conductivity, low density, less thermal mass, low dielectric constant, high specific strength and controlled permeability. [29, 30] By controlling the composition and microstructure of the porous ceramic, the properties can be tailored for their use in the specific applications.

As already mentioned in the Introduction Chapter the wide variety of applications of porous ceramics requires a broad range of porous architecture. These can be reproduced through different kinds of the fabrication process. In the following section, literature that have been collected from the research of the various groups on the fabrication of different porous structure has been summarized.

The literature review on different manufacturing methods for porous ceramics have been categorized into (a) Removal of Fugitives (b) Replica Method (c) Porous ceramics through Gelation and (d) Direct foaming method.

(a) Removal of Fugitives

Porous ceramics can be obtained by mixing appropriate amounts of sacrificial fugitives as pore forming agents with ceramic raw powder and evaporating or burning out them before or during sintering to create pores. The pore forming agents are generally classified as synthetic organic matters (polymer beads, organic fibres, etc.), natural organic matters (potato starch, cellulose, cotton, etc.), metallic and inorganic matters (nickel, carbon,

fly ash, glass particles, etc.), and liquid (water, gel, emulsions, etc.). This methodology is helpful especially for getting high open porosity. The agents, however, need to be mixed with ceramic raw powder homogeneously for obtaining uniform and regular distribution of pores. Solid fugitives such as organic materials are usually removed through pyrolysis, which requires long-term heat treatment and generates a great deal of vaporised, sometimes harmful, by-products. [7]

Y. Li *et al.* [4] fabricated porous silicon nitride with fibrous β -grain structure, using naphthalene powder as the pore-forming agent and gas pressure sintering of high temperatures above 1700°C. The bending strength of the former materials was 50–120 MPa in porosity range of 42–63% while that of the latter was 160–220 MPa in porosity of 50–54%. This substantial difference in strength is most likely due to the micro-structural difference (equiaxed versus fibrous). [4]

A. Diaz *et al.* [5] used corn starch (particle size: 5–18 μm) as a fugitive additive for fabricating porous silicon nitride ceramics. The mixture slurry was kept in under agitation for obtaining a homogeneous dispersion of the fugitives. Subsequently, the mixture was frozen and dried under vacuum. [5]

F. Chen *et al.* [31] developed equiaxed α -grains of porous silicon nitride at a relatively low temperatures (1000–1200°C) by using phosphoric acid (H_3PO_4) as the pore-forming agent and pressureless sintering techniques [31].

Zhang *et al.* [32] used mercerized cotton threads as fugitives to produce porous alumina ceramics that had continuous pores (diameter: 160 μm) aligned in one direction via the slurry coating. It was observed that by using cotton threads of different diameters he was able to get pores of different size. He used different solids concentration of the slurry and was able to fabricate porous body with varying porosity. In this case, excellent permeability was achieved

for porous ceramics with unidirectional channel pores because the gas could flow directly through the pores. [32]

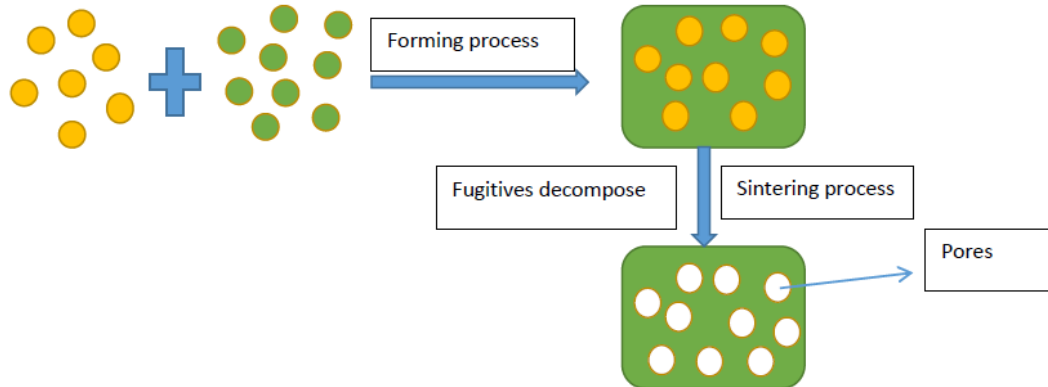


Figure 1. Removal of fugitive technique for fabrication of a porous microstructure

(b) Replica Technique

In replica technique, a cellular template is immersed or impregnated with a ceramic suspension/ precursor solution for the production of a porous ceramic having the same or the opposite morphology as that of the original porous template. Models used in this process to fabricate porous ceramics can be either natural or synthetic cellular structures. In recent years, corals, wood structures, egg shelled membranes, bacteria, have been used as natural templates. Porous ceramics with open pores in the range of 10 to 300 μm have been developed with this method at porosity levels between 25% and 95%. [1] The availability of templates exhibiting the desired microstructure, anisotropic in mechanical strength is some of its shortcomings.

Sponge replica technique is one of the best processing methods for fabrication of porous ceramics and is mostly used in industry for the preparation of ceramic filters used in molten metal filtration and other useful applications. The sponge replica technique is a novel

method to prepare open structures with pore sizes in the range of 200 μm to 3 mm. With this method, porosity in the range of 40% - 95% could be achieved. ^[1] The essential steps in this process included the adhesion of the suspension on the polymeric sponge and rheology of the slurry. Due to high pore interconnectivity, the permeability of gasses and fluids is enhanced in these porous materials. Despite being a user-friendly process, cellular structures processed through this route had very low mechanical strength due to the formation of cracked struts at the time of polymer sponge pyrolysis. ^[1]

In another method, a biphasic composite is produced which consists of a continuous matrix of ceramic precursors and homogeneously dispersed sacrificial phase. The sacrificial phase in the biphasic composite is then extracted in order to generate pores in the microstructure. The porous materials display a negative structure than that of the original sacrificial template used. This method, therefore, is in contrast to porous ceramics produced from the replica technique. The method of removal of the sacrificial template from the composite depends primarily on the type of pore former used. The different sacrificial materials used as templates can be classified as synthetic and natural organic materials. Some of these are liquids while most of them are solids. The standard extraction method of these Synthetic and natural organic materials is through decomposition which is obtained by heat treatments at higher temperatures (200°C - 1000 °C). ^[33] Liquids are generally extracted through freeze drying or sublimation after freezing. ^[34] Carbon and SiO₂ templates are removed by oxidation ^[35] and chemical leaching, ^[36] respectively. Salts are often removed by leaching with water. ^[37]

T.J. Fitzgerald *et al.* ^[37] used sodium chloride compact for producing fine open-cell SiC foams. In this process, a porous sodium chloride composite was infiltrated with Poly Carbo Silane (PCS). The preform used had a controlled particle size and density. Water was used as the leach out the salt that resulted in getting PCS foam. This was then cured by

heating in air, and finally a porous structure is obtained after pyrolysis. The structure thus formed had a homogeneous network of open pores with cell sizes varying roughly between 10 μ m and 100 μ m, with controlled relative densities. [37]

K. Schwartzwalder *et al.* [38] prepared the ceramic cellular structure of various porosities and pore sizes using a polymeric sponge. After this experiment, sponge replica technique became one of the most used methods to produce ceramics with high porosity with open pore structure. Polymeric sponge such as polyurethane (PU) [38] is the most frequently used synthetic template.

R.A. White *et al.* [39] used a novel method to preserve by duplicating the structure of corals and some marine invertebrate skeletons. For this technique, the coral is first infiltrated with wax under reduced pressure. The process produced a negative form of the cellular structure. Highly acidic solution was used to leach out the calcium carbonate based coralline skeleton. The negative template thus formed is impregnated with a ceramic suspension and by removing the organic material by pyrolysis a macro-porous ceramics is obtained. [39]

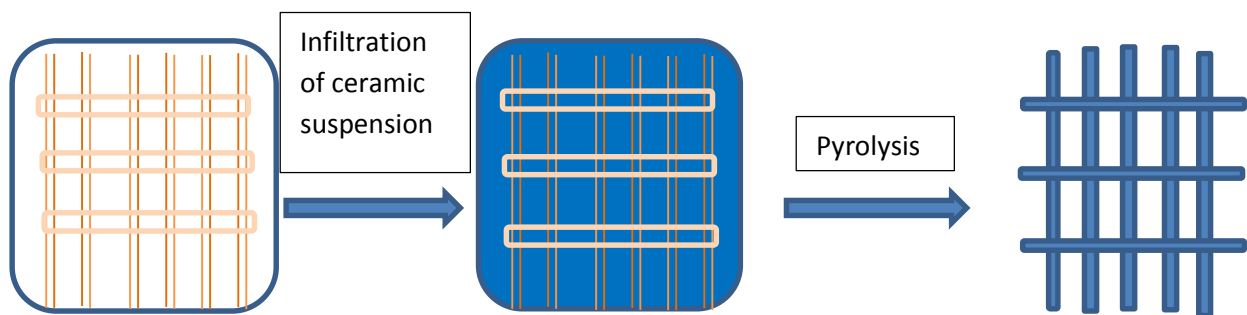


Fig. 2. Replica Technique for fabrication of porous microstructure

(c) Direct Foaming Method

The direct foaming method is a simple, quick and cheap process to prepare macroporous ceramics with porosities in the range of 40% to 97%. In this process, a ceramic suspension is infiltrated with air by using mechanical means. This process avoids the need for the pyrolysis steps before sintering. Porous ceramics fabricated from this method shows average pore sizes in the range of 35 μm to 1.2 μm . Such small pore sizes were achieved because the foams were stable for an extended period. Cell struts of the cellular structures prepared by direct foaming are dense and flawless. Thus, they usually exhibit high mechanical strength than that of structures made from replica techniques. Compressive strengths in the order of 16 Mpa was achieved even at a higher porosity level (87 % to 90 %) from porous ceramics produced from particle-stabilized wet foams. ^[21]

O. Lyckfeldt *et al.* ^[16] developed a unique method of forming process for porous ceramics. Starch was used as both consolidator/binder and pore former. Different components of porous alumina were made and de-moulded in the wet state. The porosity was found to be in the range of between 23-70%, but the samples showed excellent mechanical properties. ^[16]

M. Pradhan *et al.* ^[20] studied the effect and microstructural evolution during drying of soapnut (Reetha) based alumina foams. They concluded that setting of soapnut based foam could be achieved simply by drying without requiring any gelation step. Higher concentration of soapnut was seen to eliminate the cell size gradient throughout the thickness of the samples. The extent of cell connectivity was great and was attributed to the reduced strength of the cell wall, which ruptures during drying. ^[20]

Y Han *et al.* ^[40] studied the manufacturing of highly porous ceramics with controlled pore structure via foaming and agar gelation. Formations of macropores and window pores were induced through the process of foaming, and formation of micropores was facilitated by

adding agar. However, when the level of agar contents increased, the sizes of macropores and window pores decreased. Also, the ceramic foams prepared with higher agar contents exhibited a narrower size distribution of macropores, which was due to faster stabilization of foams via faster gelation. [40]

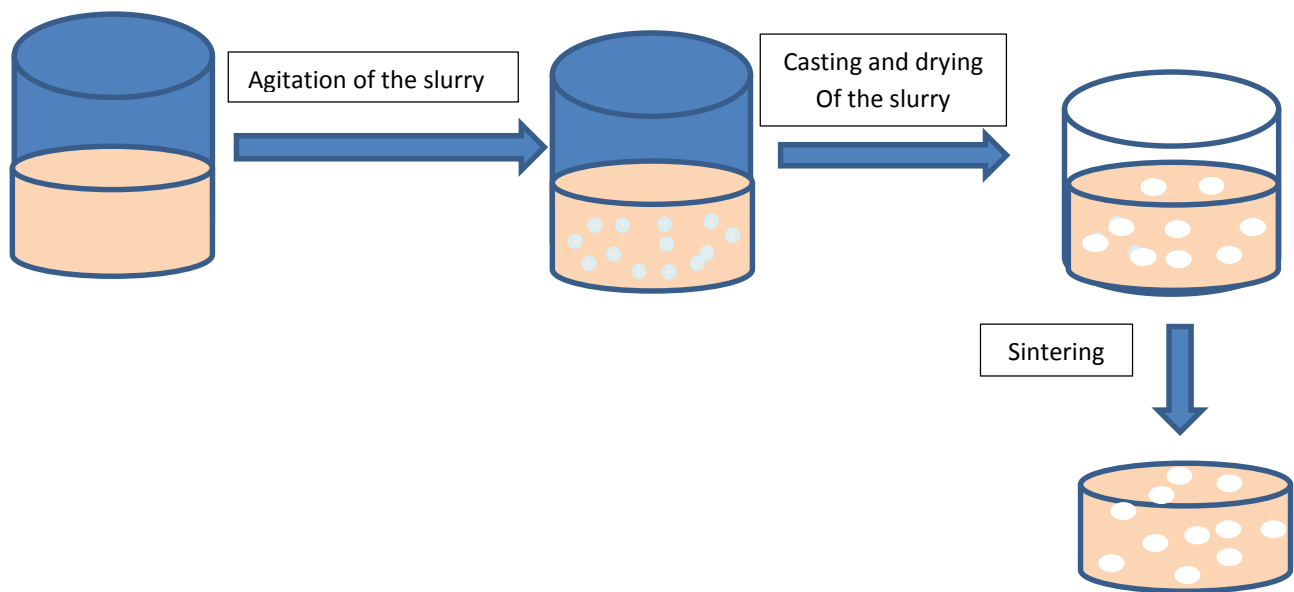


Figure -3. Direct Foaming method for fabrication of a porous microstructure

CHAPTER 3

EXPERIMENTAL DETAILS

EXPERIMENTAL DETAILS

3.1. Preparation of Natural Pore Former extract

The natural pore former extract was prepared by digesting the plant source in methanol for prolonged periods followed by drying. Water was used as the solvent for dissolving the dried mass and centrifugation of the extract was done to remove the organic residues. The obtained solution contained Glycoside.

3.1.1. Determination of Glycoside concentration

Concentrated H_2SO_4 reacts with Glycoside to form Terpene ring. This compound shows sharp absorbance at 429 nm. The percentage of Glycoside in the extract was determined by the above reaction. Standard Glycoside solution of different concentration was prepared from Glycoside (Loba Chemicals) and was used as standard solution for calibration.

3.2. Foam stability with different binders

Foam stability was studied with various adhesives and natural pore former extract. Solutions of different concentration of binder and pore former were prepared, and stirring was done for 3 hours. The foam height and liquid height were marked just after the stirring was stopped. At different time intervals, their height was marked continuously until all the foams collapsed. From the rate of liquid height change, the drainage rate was calculated.

3.3. Optimization of de flocculant concentration

Darvan C was used as a dispersant for preparing alumina slurry. For optimizing the Darvan C amount, alumina suspension was made using a different percentage of Darvan C (0.2 to 0.5) and viscosity of each suspension, was determined. The optimum concentration of Darvan C was fixed which corresponds to the minimum in suspension viscosity.

3.4. Rheological analysis

Slurries were prepared and tested for rheological behaviour to observe the effect of binder addition. The slurries were subjected to shear stress in a concentric Cylinder (Rheometer Model Rheolab, Anton Parr) at 60 shear rate and the shear stress, and viscosity were noted. The measurement was done both during up-swing (i.e. 1- 60sec⁻¹) and down-swing (60-1sec⁻¹).

3.5. Slurry preparation

Alumina slurry was prepared by two different methods of agitation: stirring and tumbling. In the stirring process, water, pore former, binder and half of required Darvan C amount was taken in a beaker. The mixture stirred with a magnetic stirrer. To its calcined alumina was slowly added in very little amount. Then remaining part of the Darvan C was added dropwise along with the constant addition of alumina. After addition of all the raw materials, the mixture was stirred for 3 hours.

3.6. Casting and Drying

Slurries made of same composition were poured into several Vaseline-coated low-cost plastic tea cups. They were then set to dry in preheated oven at different temperatures. The optimum drying temperature was determined, and slurries were dried at the optimized temperature.

3.7. Sintering

Sintering of the green samples was done at 1500°C for 2 hours according to the following schedule:

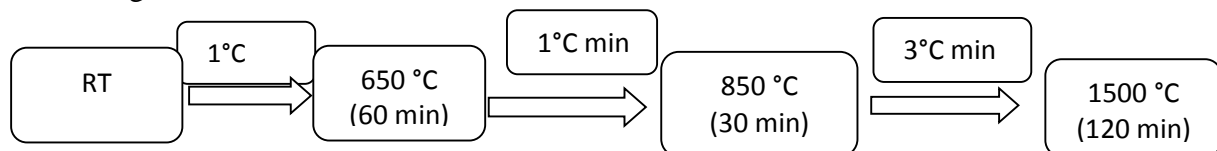


Figure 4. Time Schedule of Sintering of Samples at 1500°C

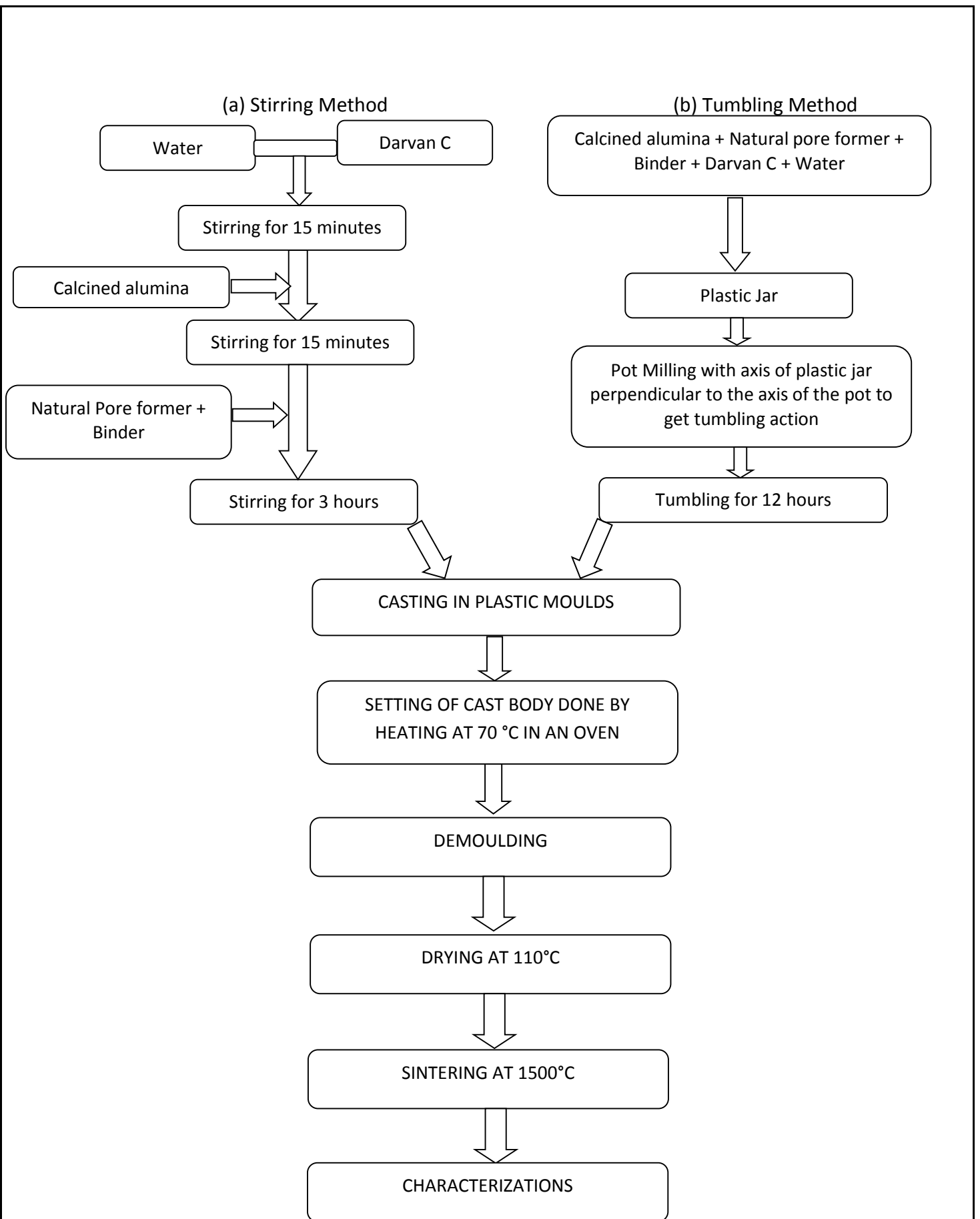


Figure 5. Flow chart related to slurry preparation (a) Stirring method (b) Tumbling method

3.8. Characterizations

3.8.1 Apparent Porosity and Bulk Density

The apparent porosity and bulk density of sintered samples were measured by Archimedes principle for each batch. The dry weight of the samples was taken and then samples were immersed in water in a glass beaker. Then the glasses were kept inside the vacuum desiccator and evacuated till bubbles stopped coming out of the samples. The suspended and soaked weights were taken for each batch.

Apparent porosity and Bulk density were calculated by the following formulae ^[41]:

$$\text{Apparent Porosity} = (S - D) / (S - W) \quad [1]$$

$$\text{Bulk Density} = D / (S - W) \quad [2]$$

Where, D = Dry weight, W = Soaked weight, S = Suspended weight

3.8.2 Total porosity and Closed porosity

The total porosity and closed porosity of the samples were calculated using the formula ^[41]:

$$\text{Total Porosity} = 1 - \frac{B.D}{T.D} \quad [3]$$

$$\text{Closed Porosity} = \text{Total porosity} - \text{Apparent porosity} \quad [4]$$

3.8.3. Optical Microscope microstructure

The selected sintered samples were viewed under an optical microscope. The images were taken using Olympus optical microscope fitted with a CCTV camera using Image analysis software. The images were taken at 500X magnification. The samples were placed under the microscope and then viewed through the monitor screen. The samples prepared with PVA as a binder were chosen for optical imaging.

3.8.4 Measurement of compressive strength

The cold crushing strength of the samples was measured using Universal testing machine (UTM) Model H10KS Tinius Olsen. The crosshead speed was 0.5 mm/min and load shell used were of 1 KN and 10 KN. The cylindrical samples were broken by applying compressive force and CCS was calculated using the following formula ^[41].

$$\text{CCS (MPa)} = \frac{P}{A} \quad [5]$$

Where, P = Maximum Load. A = Area of cross section of samples

3.8.5. FESEM microstructure

The microstructure and porosity of porous HA samples were studied by Field Emission Scanning Electron Microscope (FESEM). The samples were gold coated for 3 minutes prior in FESEM machine (FEI NANO SEM 450). They were observed in secondary electron (SE) mode at 10 KV accelerating voltage.

CHAPTER 4

RESULTS AND DISCUSSION

4.1. Determination of concentration of Amphipathic Glycoside (AG) in the Natural pore former extract

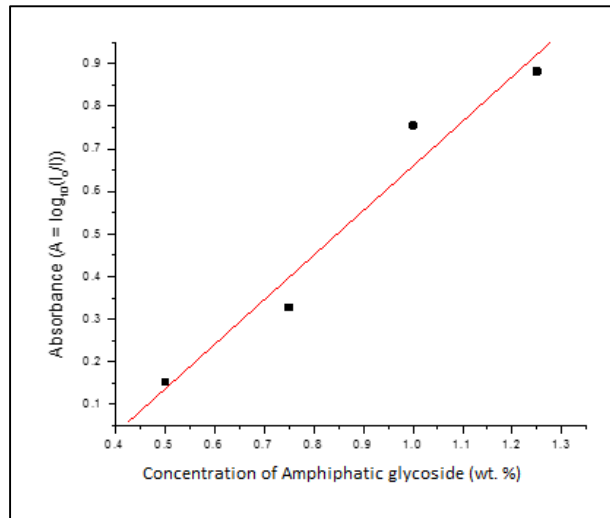


Fig 6. Standard curve for determination of AG obtained using UV-Visible Spectrophotometer

The absorbance of the extract was measured (at 429 nm) and plotted against the standard curve that gave 0.53. From the calibration graph, the concentration of AG in the extract was found to be 6.4 % AG.

4.2. Comparison of liquid drainage rate with different binder

From Table 1 it can be observed that an increase in the concentration of pore former increases the foam volume. It also shows that with a rise in the Guar Gum concentration higher foam stability can be achieved followed by sucrose, PVA and Mahua (*Madhuca Longifolia*). Mahua being a natural binder was used first for the preparation of the sample. Though we were able to prepare extract by digesting the plant matrix in water, the very short shelf life of the extract posed a hindrance to its use as a binder. It would decompose within 2 – 3 days. So it was not used as the binder in our further work. Higher Guar Gum concentration (7 %) resulted in a highly viscous slurry the slurry becomes highly viscous. As

a consequence, the maximum solid loading was only 20 vol. % with no workable pourability. Therefore, next trials were conducted with sucrose and PVA as binder for the preparation of samples with different pore former concentration and binder concentration with an aim to achieve as high solid loading as possible with acceptable limit of interconnected porosity.

Table 1- Drainage rate of liquid with different binder (Sucrose, PVA), varying their concentration with various AG combination

Binder type	Binder (Wt. %)	Natural pore former (Amphipathic Glycoside wt. %)	Drainage rate (μl/min)
No binder	-	2	833.33
MAHUA (<i>Madhuca longifolia</i>)	10	2	214
	20	2	136.36
GUAR GUM	0.2	2	266.4
	0.3	2	175
	0.4	2	142
	0.5	2	112.64
	0.6	2	78.3
	0.7	2	52.5
SUCROSE	10	2	250
	40	2	125
	50	2	102
	40	5	185
	50	5	120
	60	5	111
	70	5	85
PVA	8	2	90.9
	10	2	55.5
	3	5	142
	5	5	121
	7	5	79
	10	5	57

4.3. Particle size analysis of Calcined Alumina

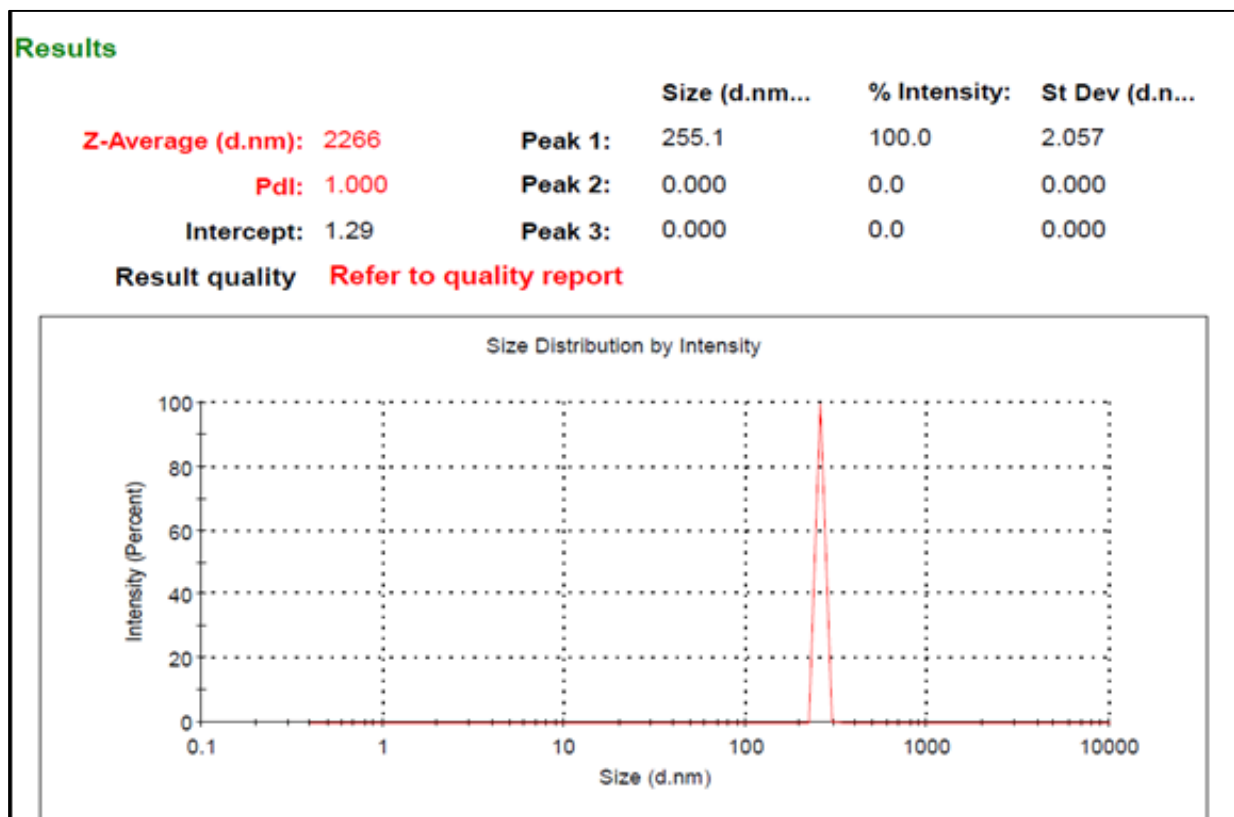


Figure 7. Particle size distribution of calcined alumina

Figure 7. Shows the particle size distribution of as received alumina. The particle size distribution is essentially mono modal, and average particle size is 0.28 μm .

4.4. Optimization of Deflocculant Concentration

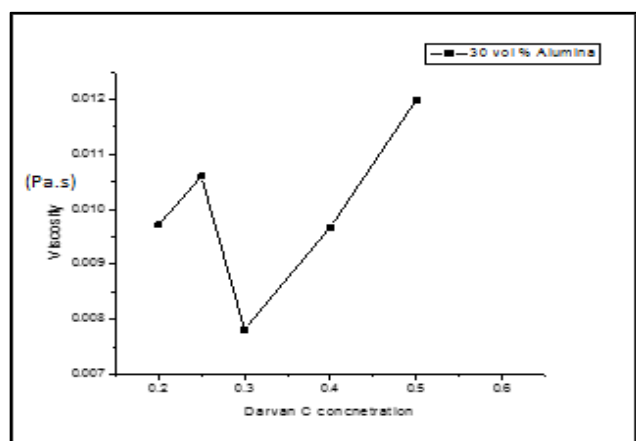


Figure 8. Viscosity at different Darvan C concentration

Figure 8 shows the viscosity of alumina slurry as a function of de flocculant concentration (Darvan C). The plot shows that the minimum viscosity of the slurry is achieved at 0.3 Wt. % Darvan C addition with respect to alumina. Beyond 0.3 Wt.%, the viscosity increases due to overcrowding and compression of the double layer. Therefore in this study a fixed amount of Darvan C (0.3 Wt. %) was added to alumina slurry. It was also observed that a change in solid loading did not alter the de flocculant percentage for maximum fluidity.

4.5. Rheological study of Alumina Slurry

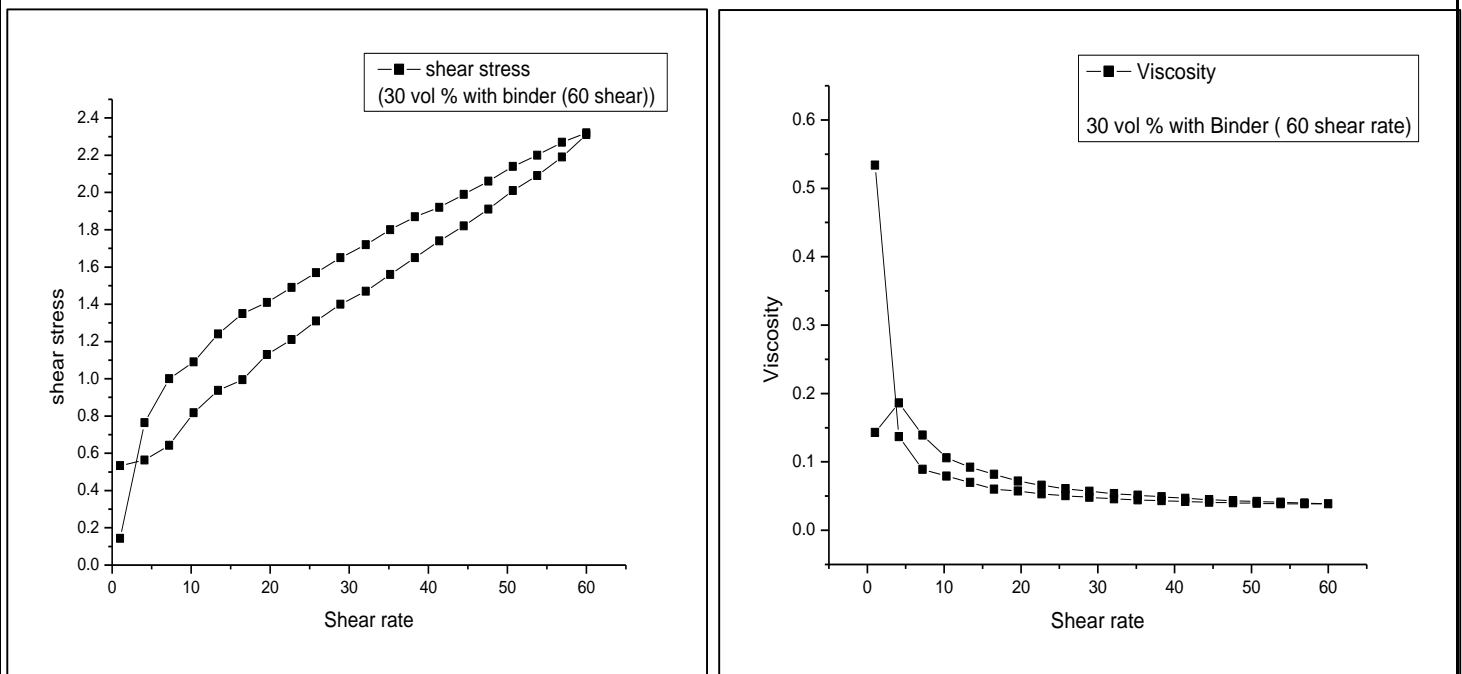


Figure 9- Rheological behaviour of alumina slurry with binder

Figure 9 shows the stress-shear rate behaviour of an alumina slurry. The substantial loading was 30 vol. %. The shear stress rate curve shows a typical shear thinning behaviour with a hysteresis between the upswing and downswing curve. The viscosity curve, shows that a decreases in the viscosity with the increase in shear rate, and a steady state viscosity of

0.08 Pa. s is obtained at 30 s^{-1} . A very little change in viscosity is observed at higher shear rate.

4.6. Samples with Sucrose as binder and Amphipathic Glycoside extract

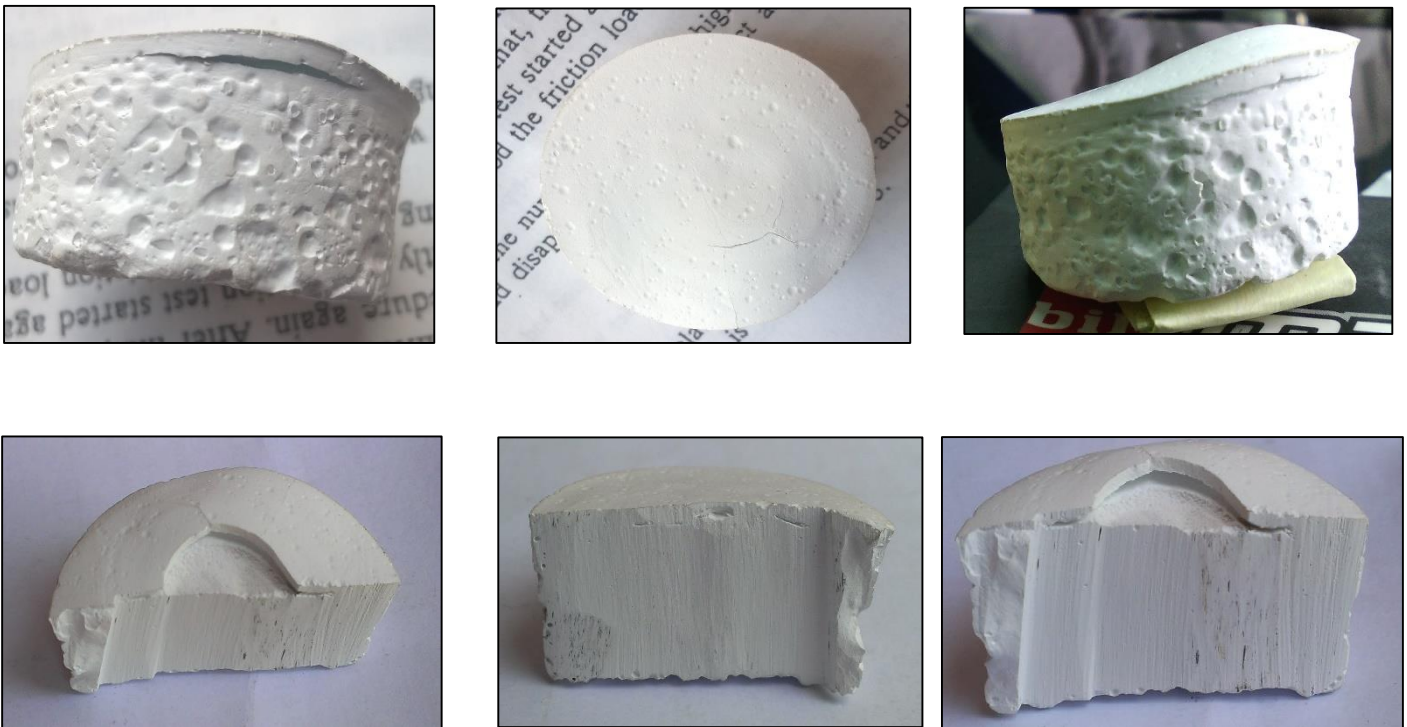


Figure 10. Photographs of sample with Sucrose as binder and Amphipathic Glycoside extract

Samples were prepared with 30 vol. % solid loading, 70 Wt. % sucrose as a binder, and 2 Wt. % pore former. During drying of the samples, a layer of liquid appeared on the surface after one day. This indicated settling of the particles and instability of foams. The presence of liquid at the top resulted in long drying time and differential drying. Probably the release of structural water contributed to the higher liquid content. The dried sample was, therefore dense, and cracks were observed at the surface after sintering. When the sample was cut open into two halves, it showed that there was no pore in the bulk of the sample. The fine pore present in the samples were because of the binder (sucrose) burnout. The surface isolated

pores were because of long drying time caused by the expulsion of water from sucrose and formation of a dense sample instead of a porous sample were the reason to use PVA as the binder.

4.7. Samples prepared with PVA as binder and Amphipathic glycoside (AG)

4.7.1. Trial sample made with PVA as binder and AG as pore former



Fig 11. Photograph of the trial sample prepared with 35 vol. % solid loading, 5 % PVA, 0.1 % Pore former and 0.3 % Darvan C

As a first trial two alumina slurry (30 vol. % and 35 vol. %) were first prepared on a trial basis. 5 % PVA, 0.1 % pore former and 0.3 % Darvan C were added to slurry. After 3 hours of stirring, the slurries they were casted into Vaseline coated plastic tea cups and were oven dried at 40 °C in an oven. After 5 days of drying, the samples were taken out and sintered at 1500°C. Fig. 11 shows the camera photograph of 35 vol. % solid loading samples. It can be seen that the sintered sample had a hollow structure. Due to long drying period (4 days) the foam coalescence might have taken place which resulted in a bigger foam and, as a result, a structure with a large pore has formed. This called for the optimisation of drying temperature, binder and pore former concentration which is reported in the following section.

4.7.2. Optimization of the drying temperature

Results of section 4.7.1 showed that long drying time permitted foam segregation and liquid drainage. Therefore, optimization of drying temperature was done. Alumina porous

sample were prepared by Slurry Casting method using 2 % pore former. 30 vol. % solid loading, 0.3 % Darvan C and 5% PVA were used as the de flocculant and the binder respectively. The alumina slurry was prepared by a stirring method using a magnetic stirrer. After the slurry had been prepared, the stirring was continued for 3 hours for the generation of foams in the slurry. The slurries was cast in a low-cost plastic tea cup [diameter =21 mm and height= 15mm]. The cast slurries were dried at different temperature (50°C, 60°C, 70°C, and 80°C) for setting. The setting of the cast body was due to combined action of water removal and hardening of the binder. The photographs of the surface of the dried cast body are shown in Figure-12. The surface shown in the photograph is the bottom surface of the samples. It can be seen that when drying temperature increases from 50°C to 80°C the pore size increases (Fig 12 (a) to 12 (d)). Therefore, for a finer pore size a lower drying temperature is preferable. But a low drying temperature resulted in a very long drying time (more than 4 days) for easy drying and de-moulding of the samples. This long drying resulted in foam instability and liquid drainage. The differential liquid content at the top and bottom surface of the cast resulted in the differential drying between top and bottom surface and cracking of the cast body. (Fig 13). This type of cracking behaviour was also observed by Pradhan *et al.* ^[41]

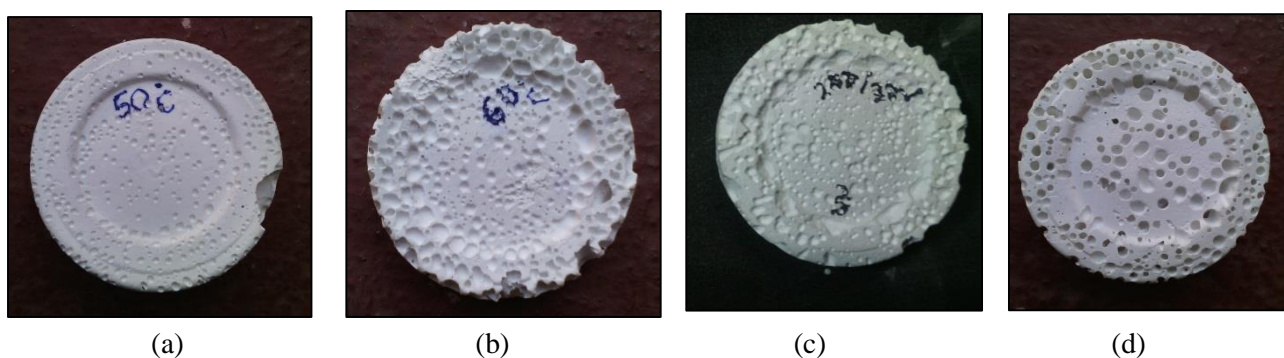


Fig.12. Bottom surface of the samples dried at (a) 50°C (b) 60°C (c) 70°C (d) 80°C

In this study, it was also further noted that little foam stability and long drying time resulted in foam migration and foam collapse. Thus, the foam at the top surface collapsed giving rise to a less porous surface at the top and more porous surface at the bottom. It was also observed that the lower surface foams could not escape may be because of possible settling of the alumina particles and attachment of foams to the particles. A relatively small porous cast was observed at the top surface (Figure 13). This kind of two-layer structure or hierarchical pore structure was found in many samples. The results indicate that there is a further possibility for drying time optimization. Low-pressure drying or vacuum drying may be one such option.



Fig.13. Samples Prepared by Stirring method shows gradient in pore size from top to bottom

The literature review suggested that such behaviour can be avoided if foam can be attached to the particles. It was further thought that the stirring action of relatively higher intensity was probably because foam detachment and foam coalescence. In order to overcome these two issues, it was decided to change the foaming part to a slow process (Tumbling Method).

4.7.3. Alumina Slurry preparation by Tumbling Method

The batch was put in a plastic bottle and fixed in a porcelain jar such that, the rotational axis of the jar and that of the pot were in the perpendicular direction. Thus, when

the mill was rotating along with the pot, the plastic lined jar was tumbling along its length, giving rise to a higher tumbling effect and pore generation. However, due to the lower rotational speed of the jar and the bottle, the tumbling action was a slow process, and this allowed a uniform distribution of pore within the slurry (Figure 14).

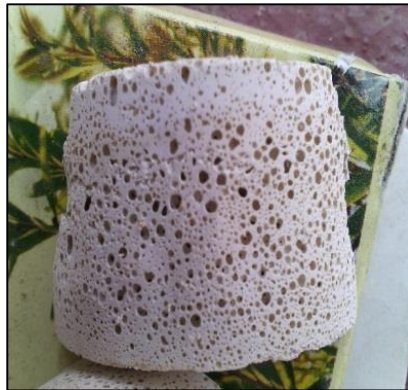


Fig.14. Samples Prepared by tumbling method shows more uniformity in pore distribution.

4.7.4 Effect of slurry preparation method on the nature of porous sample formed.

As already mentioned, the porous sample was prepared by two different methods, Stirring Method and Tumbling Method. The results suggested that even when the other parameters (such as solid loading, amount of binder and pore former) were kept same, the macro and micro structure that were produced by the two methods were different. Fig.13 and Fig. 14 shows the camera photograph of the samples prepared by Stirring and Tumbling method respectively. While the Stirring Method has produced samples with irregular distribution of pores, tumbling process has produced a relatively more uniform porous structure. Samples prepared by former method were cracked at the top side, which indicate differential drying resulting from drainage of the foam during the setting of the samples. No such defects were observed in the tumbling method sample. It can be argued that the difference in the structure is because of the difference in substantial loading (25 vol. % for

stirring method and 35 vol. % for tumbling process). It is possible that a higher solid loading in the samples prepared by stirring way could have produced a crack free and homogeneous microstructure. The same logic can be refuted by comparing the optical microstructures of the samples prepared by the two methods (stirring process and tumbling method) for identical substantial loading, binder, and pore former content. (Fig. 15)

Figure 15. (a) and (b) show the optical microstructures of two such samples where the solid loading was 35 vol. % along with 5 % binder and 3 % pore former. It can be clearly seen that in the samples produced by the stirring method, pores can be considered as a mixture of open and closed pores. The open pores were also found to be mostly isolated, and the number of closed pores is more than the number of open pores. On the other hand, Tumbling Method samples hardly show any closed pore, and all the pores are interconnected. At some isolated places thinning down of the struts could also be seen which indicate that the solid loading could be further improved in Tumbling Method. Thus, the microstructure clearly shows that the slurry preparation method has a profound effect on the ultimate microstructure of the porous sample.

The foam that are produced in the stirring method is due to stirring effect that is a relatively high energy process. This process not only produces the foams, but the continuous agitation probably disturbs the created foams and prevents them from getting attached to the particles leading to the coalescence of pores leading to pore migration and pore instability. The tumbling method is a relatively slow process where the foams are generated due to tumbling action of slurry with grinding media for a relatively high vol. % of solid loading (35 vol. % in this case). This low energy process permits the foam to get attached to the particle so that the foams are not only stable but also it is uniform throughout the slurry, and the

coalescence effect is least or minimum. The samples produced in this method have mostly interconnected pores and uniformly porous microstructure.

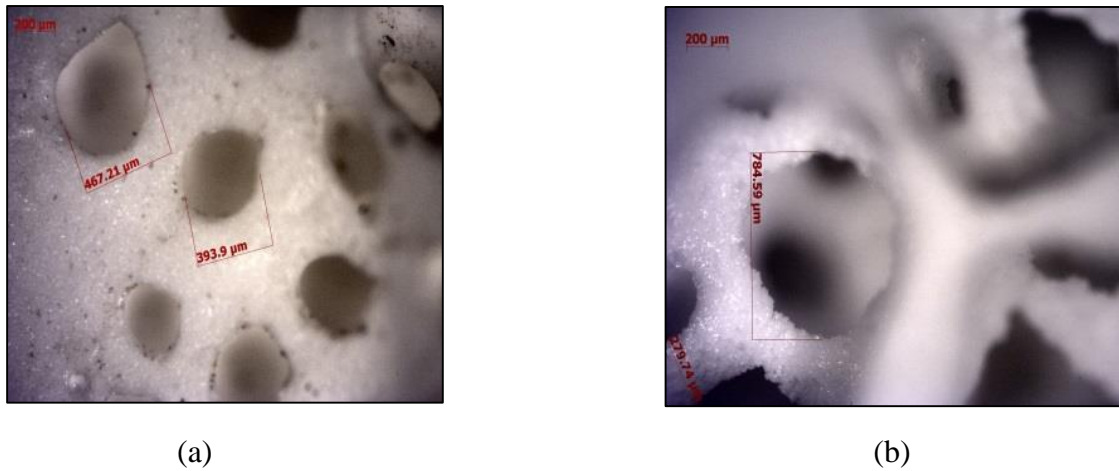


Fig .15. Optical Microscope microstructure of
(a) 35 vol. % solid loading + PVA 5 % + pore former 3 % in stirring method
(b) 35 vol. % solid loading + PVA 5 % + pore former 3 % in tumbling method

4.8. Effect of glycerol addition on the microstructure development in porous alumina

In this study, the concentration of PVA (used as binder) was varied along with the concentration of the pore former. Two different ways of mixing was used; stirring and tumbling. Glycerol, (0.5g/l) was additionally added in the slurry to increase the foam stability.

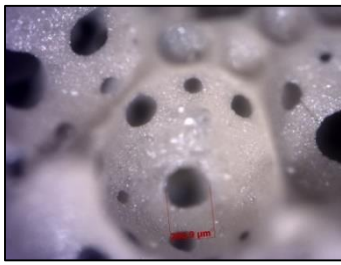
4.8.1. Variation of porosity and strength with change in pore former concentration

In the above section of foam stabilization, it is seen that there is an increase in the amount of foam generated as pore former concentration increases. But as can be seen from Table 3 (sample 1, 2, 3), with the increase in pore former concentration, the porosity is decreasing. Generally with the increase in solid loading, the porosity decreases due to the

settling of particles. Here in all the three samples the solid loading was kept constant i.e. 30 vol. %. Normally with Darvan C the pH of the slurry is >9.5 . This helps the particles remain deflocculated in the slurry (IEP of Al_2O_3 is at pH 7-8). But with the increase in the pore former (pH=4) concentration the pH of the slurry is brought down closer to IEP value which might be one of the reasons for particle settling during the setting of the cast. Therefore, the effect of pH causes foam instability and results in a sample which has a dense body with foam residing in one part and not the whole body.

At low pore former concentration, the pores are uniformly distributed as there is less particle settling. This leads to the formation of a more open structure with high apparent porosity (Table 2, sample 1). The samples with low pore former concentration had a thick strut (Fig. 16 (a)) which increase the crushing strength than the samples with high pore former level. As stated above, with the rise in pore former, the amount of foam generated increases as well as rate particle settling increases (pH effect). This leads to the non-uniform distribution of pores in higher pore former containing samples with some parts of the body being sufficiently dense (Fig 16 (b)) whereas large pores remain in some other parts. This leads to the failure lead to failure of the sample at very low load (Table 2, Sample 3). These defects (large pores) might the reason for the lower breaking load of failure of high pore former containing samples.

From the optical images, it can be seen that there is no interconnection between the pores (Fig. 16). So there was a need to stabilise further the foam by increasing the contact between the particle and foams. This prompted us to add Glycerol, which is known to increase foam stability by changing the interfacial energy between the particles. ^[21] Samples were prepared with low pore former extract along with glycerol at different solid loadings and binder concentration. The slurries were prepared by two methods: stirring and tumbling.



(a)

(b)

(c)

Fig 16. (a) 30 vol. % with 1.5 % pore former, (b) 30 vol. % with 3 % pore former
(c) 30 vol. % with 4.5 % pore former

4.8.2 Variation of porosity and strength with variation in solid loading and binder (PVA) concentration

To study the variation of porosity and strength with solid loading and binder (PVA) concentration, the pore former concentration was kept constant at 3 %. The reason for this low level of pore former has been discussed above. The solid loading was varied from 25 vol. % to 35 vol. % and the PVA concentration used was 3 % and 5 % along with the addition of glycerol. A higher solid loading, porosity increases due to greater degree of pore attachment with the particles which can be seen in the optical microscope microstructure [Fig (18 (a) and Fig 18 (b))]. The concentration of binder also played a significant role in the foam stability. It was also observed that with the increase in binder concentration the particle–particle distance increases which are because of the formation of comparatively large pores and increase in porosity (Fig. 17).^[42]

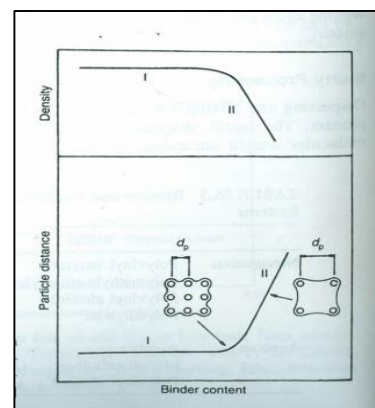


Fig. 17. Effect of Binder content on particle separation in green body. At higher binder content, particles are separated far apart which result in higher porosity in the sintered samples

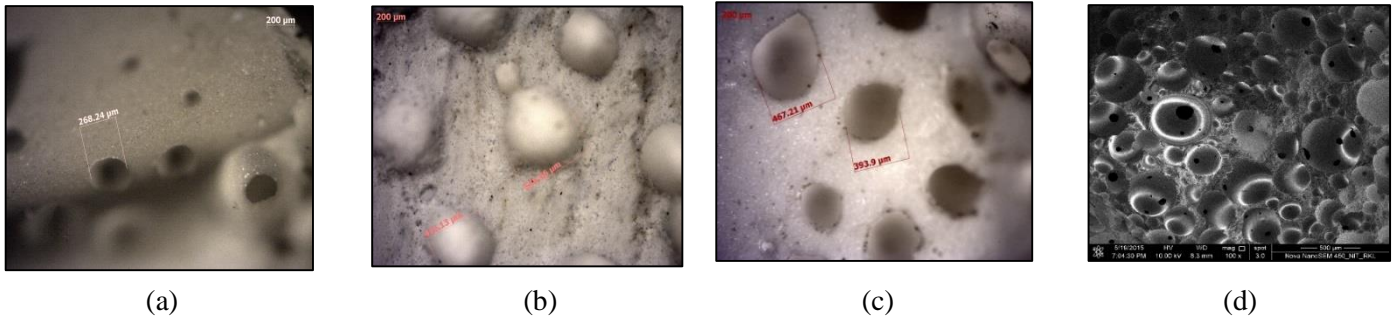


Fig 18. (a) 25 vol. % with 5 % PVA and 3 % , (b) 30 vol. % with 5 % PVA (c) 35 vol. % with 5% PVA (d) Microstructure of sample made from 35 vol. % solid loading, 3 % pore former and 5% PVA showing interconnection between pores

Table 2 -Summary of Apparent porosity, Total Porosity, Closed porosity, Bulk Density and CCS of the samples prepared with different concentration of PVA as Binder and AG

Foaming method	Alumina (vol. %)	PVA (Wt. %)	Natural pore former extract (Wt. %)	Apparent porosity (Wt. %)	Bulk density	Total porosity	Closed porosity	Strength (MPa)
Stirring Method	30	1.5	3	60.56	1.49	62.56	2.00	2.004
	30	1.5	4.5	48.41	1.58	60.30	11.89	1.495
	30	1.5	6	43.51	1.81	54.52	11.01	0.568
Stirring Method (with Glycerol)	25	3	3	41.14	1.86	53.26	12.12	6.325
	30	3	3	46.22	1.61	59.54	13.32	4.012
	35	3	3	52.17	1.47	63.06	10.89	0.412
	25	5	3	39.13	1.76	55.77	16.64	2.987
	30	5	3	45.26	1.55	61.05	15.79	1.786
	35	5	3	57.32	1.37	65.57	8.25	0.887
Tumbling Method (with Glycerol)	25	5	1.5	40.64	1.98	50.25	9.61	12.467
	30	5	1.5	47.24	1.73	56.53	9.29	5.565
	35	5	1.5	56.81	1.54	61.30	4.49	4.859
	25	5	3	46.36	2.01	49.49	3.13	5.46
	30	5	3	51.17	1.61	59.54	8.37	0.65
	35	5	3	69.58	1.17	70.60	1.02	0.755

4.8.3. Variation of microstructure with change in pore former concentration and solid loading: -

Fig. 19 shows that with the increase in pore former level, the size of the pores increases. Further, it was also observed that number of pores per unit volume of the samples were more in case of Fig 18 (b) than Fig. (a). In the foam stabilisation section, it was seen that more foams were generated when the pore former concentration was increased. This idea leads us to the conclusion that the increase in pore size with an increase in pore former level might be due to the coalescence of the smaller pores generating a bigger pore. With higher solid loading, more foams get stabilised and hence there is an increase in porosity and interconnection between them as seen from Fig. 18 (a) and Fig. 18 (b).

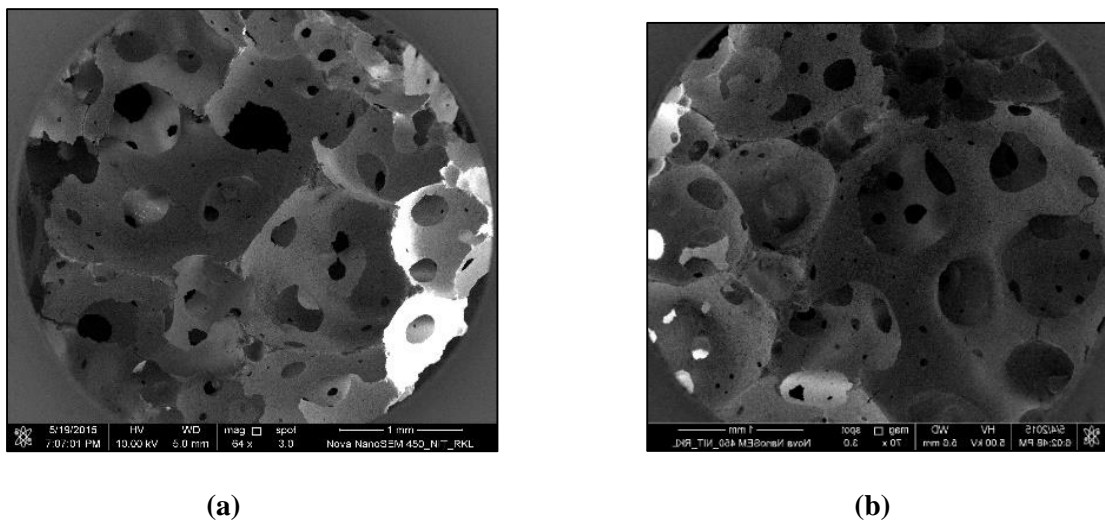


Fig 19. FESEM microstructure of (a) 35 vol. % alumina, 1.5 % pore former, 5 % PVA (b) 35 vol. % alumina, 1.5 % pore former, 5 % PVA . The pore fraction, porosity and the interconnectivity increases with the increase in the pore former

CHAPTER 5

CONCLUSIONS
AND
SCOPE OF FURTHER WORK

CONCLUSIONS

The present study on the processing of porous alumina using natural pore former dealt with the treatment and fabrication aspect of porous ceramics using a natural pore former containing amphipathic glycoside as a pore-forming compound. No previous report on the utilization of this natural pore former could be found in the literature. The conclusion that can be drawn from this preliminary study is as follows-

- ❖ This study proves that this amphipathic glycoside-containing natural pore former are quite active in producing porous ceramics.
- ❖ The slurry preparation method has an effect on the porosity and pore structure of porous ceramics.
- ❖ It was observed that the Tumbling Method of slurry preparation produced a more homogeneous porous structure as compared to the stirring method.
- ❖ Tumbling method samples with a combination of 35 vol. % solid loading and 5 % PVA, 3 % pore former could produce interconnected pores with a pore size in the range 400 μm – 600 μm and total porosity around 70 %.
- ❖ A higher PVA content, the crushing strength of the porous samples decreases because of increased particle content resulting in higher porosity. 1.5 % pore former was not effective in producing an effective interconnected pore. Rather produced a closed pore array.
- ❖ The addition of 0.5 ml/l of glycerol to the slurry helped in increasing the foam stability and porous structure.
- ❖ The foam stability was affected by the addition of Binders and Guar Gum, and PVA produced to be a better foam stabilizers as compared to Mahua extract and sucrose.

SCOPE OF FURTHER WORK

- ❖ The foam stability needs to be studied in detail using different concentration of pore formers, various types of binders, surfactants and solid loading.
- ❖ The drying temperature needs to be further optimized for getting a broad range of pore size. Some of the options are freeze drying and vacuum drying.
- ❖ This study was concentrated on medium solid loading (25-30 vol. %). The entire spectrum of the solid loading need to be tried (10 – 50 vol. %) to see the effect of solid loading on porosity, pore structure and strength of the porous materials.

REFERENCES

1. A. R. Studart, U.T. Gonzenbach, E. Tervoort and L. J. Gauckler, “Processing Routes to Macroporous Ceramics: A Review”, *J. Am. Ceram. Soc.* 89 [6] 1771-1789 (2006).
2. H. C. Quing, X. Zhang, J. E. Caittan, S. Mong and S. Du “Synthesis , Microstructure and Properties of high strength porous ceramics”, *Ceramic Materials- Progress in Modern Ceramics* (2012).
3. www.intechopen.com.
4. Y. Li, F. Chen, L. Li, W. Zhang, H. Yu, Y. Shan, Q. Shen and H. Jiang, “Gas Pressure Sintering of Arbitrary Porous Silicon Nitride Ceramics with High Mechanical Strength”, *J. Am. Ceram. Soc.* 93 [6] 1565–1568 (2010).
5. A. Diaz and S. Hampshire, “Characterisation of porous silicon nitride ceramics produced with starch”, *J. of Eur. Ceram. Soc.* 24 [2] 413-419 (2004).
6. J.H. Eom, Y.W. Kim and S. Raju, “Processing and Properties of macroporous silicon carbide ceramics: A review”, *J. of Asian Ceram. Soc.* 1 [3] 220-242 (2013).
7. T. Ohji and M. Fukushima, “Macroporous ceramics: Processing and Properties”, *International Materials Reviews* (2012).
8. T. Ota, M. Imaeda, H. Takase, M. Kobayashi, N. Kinoshita, T. Hirashita, H. Miyazaki and Y. Hikichi, “Porous Titania Ceramic Prepared by Mimicking Silicified Wood,” *J. Am. Ceram. Soc.*, 83[6] 1521–3 (2000).
9. M. Mizutani, H. Takase, N. Adachi, T. Ota, K. Daimon and Y. Hikichi, “Porous Ceramics Prepared by Mimicking Silicified Wood,” *Sci. Technol. Adv. Mater.* 6[1] 76–83 (2005).
10. J. Saggio-Woyansky, C. E. Scott and W. P. Minnear, “Processing of Porous Ceramics,” *Am. Ceram. Soc. Bull.*, 71[11] 1674–82 (1992).

11. P. Colombo, E. Bernardo and L. Biasetto, "Novel Microcellular Ceramics from a Silicone Resin," *J. Am. Ceram. Soc.*, 87[1] 152–4 (2004).
12. S. Dhara and P. Bhargava, "A Simple Direct Casting Route to Ceramic Foams," *J. Am. Ceram. Soc.*, 86[10] 1645–50 (2003).
13. T. Tomita, S. Kawasaki and K. Okada, "A Novel Preparation Method for Foamed Silica Ceramics by Sol–Gel Reaction and Mechanical Foaming," *J. Porous Mater.* 11[2] 107–15 (2004).
14. Sepulveda, P. Binner and J.G.P, "Processing of cellular ceramics by foaming and in-situ – polymerization of organic monomers." *J. of Eur. Ceram. Soc.* 19 [12] 2059-2066 [1999].
15. F.S. Ortega, P. Sepulveda and V.C. Pandolfelli, "Monomer Systems for gel casting of foams", *J. of Eur. Ceram. Soc.* 22 [2] 1395-1401 (2002).
16. O. Lyckfeldt and J.M.F. Ferreira, "Processing of porous ceramics by starch consolidation," *J. of Eur. Ceram. Soc.* 18, 131 -140 (1998).
17. V.F. Janas and K.S. Tenhuisen, "Viscous Suspension: Spinning process for Producing resorbable ceramics fibers and scaffolds," U.S. Patent, US6451059B1, (2002).
18. M.F. Sanches, N. Vitorino, C. Freitas, J. C.C. Abrantes, J. R. Frade, J.B.R. Weta and D. Hotza "Cellular ceramics by gelatin gel casting of emulsified suspensions with sunflower oil," *J. of Eur. Ceram. Soc.* 35 [9] 2577- 2585 (2015).
19. L.Y. Yin, X.G. Zhou, J. S. Yu, H. Wang and Z. Liu "Protein forming method to prepare Si_3N_4 foams by using a mixture of egg white protein and "Whey" protein isolate," *Ceram. International*, 40, 11503-11509 (2014).
20. M. Pradhan and P. Bhargava, "Defect and microstructural evolution during drying of soapnut based alumina foams", *J. of Eur. Ceram. Soc.* 28 (2008) 3049-3057.

21. U.T. Gozenbach, A. R. Studart, E. Tervort and L.J. Gauckler, "Macroporous Ceramics from Particle Stabilized wet foams," J. Am. Ceram. Soc. 90 [1] 16 -22 (2007).
22. U.T. Gozenbach, A. R. Studart, D. Steinlin E. Tervort and L.J. Gauckler, "Processing of particles stabilised wet foams into Porous ceramics," J. Am. Ceram. Soc. 90 [11] 3407-2414 (2007).
23. Q. Fu, M.N. Rahaman, F. Dogan and B.S. Bal, "Freeze casting of porous hydroxyapatite scaffolds. I. Processing and general microstructure," J. Biomed. Mater. Res. B 86 (2008) 125–135.
24. S. Deville, E. Saiz and A.P. Tomsia, "Freeze casting of hydroxyapatite scaffolds for bone tissue engineering," Biomaterials 27 5480–5489, (2006).
25. Wai-Yee Yeong, Chee-Kai Chua, Kah-Fai Leong and Margam Chandrasekaran, "Rapid prototyping in tissue engineering: challenges and potential", TRENDS in Biotechnology [22] No.12 (2004).
26. "Handbook of Advance Ceramics: Materials, Application and Properties," Edt – S. Somiya, page- 1131.
27. Y. Guzman, "Certain principles of formation of porous ceramic structures, properties and application (a review)," J. Por. Mat. [9] 28-31, (2003).
28. E.J.A.E. Williams, J.R.G. Evans, "Expanded ceramic foams", J. Mat. Sci. 31 (1996) 559-563.
29. U. Soy, A. Demir, F. Caliskan, "Effect of Bentonite addition on the fabrication of reticulated porous SiC ceramics for Liquid Metal infiltration," Ceram. International,37 [1] 15-19 (2011).
30. M.A. Alvin, T.E. Lippert, J. E. Lane "Assesment of porous Material for hot gas filtration applications," J. Am. Ceram. Soc. Bull. 70 (9)1491-1498 (1991).

31. F. Chen, Q. Shen, F. Yan and L. Zhang, "Pressureless Sintering of α -Si₃N₄ Porous Ceramics Using an H₃PO₄ Pore-Forming Agent," J. Am. Ceram. Soc. 90 (8) 2379-2383 (2007).
32. J.-F. Yang, G.J. Zhang and T. Ohji, "Fabrication of Low-Shrinkage, Porous Silicon Nitride Ceramics by Addition of a Small Amount of Carbon", J. Am. Ceram. Soc., 84 (2001) 1639–41.
33. S.H. Lee and Y.W. Kim, " Processing of cellular SiC Ceramics using polymer microbeads "J. Korean Ceram. Soc. 43, 458–462 (2006).
34. M. Fukushima, M. Nakata, Y. Zhou, T. Ohji and Y. Yoshizawa, "Fabrication and properties of ultra highly porous silicon carbide by the gelation freezing method " J. Eur. Ceram. Soc., 30, 2889–2896 (2010).
35. H. Wang, I.Y. Sung, X.D. Li and D. Kim, J. Porous Mater, "Fabrication of porous SiC ceramics with special morphology using sacrificing template method" 11, 265–271 (2004).
36. Q.D. Nghiem, A. Asthana, I.K. Song and D.P. Kim, "Fabrication of porous SiC-based ceramic microchannels via pyrolysis of templated preceramic polymers" J. Mater. Res., 21, 1543–1549, (2006).
37. T.J. Fitzgerald, V.J. Michaud and A. Mortensen, "Processing of Microcellular SiC Foams. Part 2: Ceramic Foam Production", J. Mater. Sci, 30, 1037–1045, (1995).
38. K. Schwartzwalder, A. V. Somers, "Method of Making Porous Ceramic Articles", US Patent 3,090,094 (May 21, 1963).
39. R. A. White, E. W. White, and J. N. Weber, "Replamine form—New Process for Preparing Porous Ceramic, Metal, and Polymer Prosthetic Materials," Science, 176 [4037] 922 (1972).

40. Y. Han, J. Choi, H.S. Kim, H. Kim, J. Park, "Control of pore and window size of ceramic foams with tri-modal pore structure: Influence of agar concentration." *Materials Letters*, Vol. 110, 1 (Nov.2013) 256-259
41. ASTM International, C830 - 00(2011) , Standard Test Methods for Apparent Porosity, Liquid Absorption, Apparent Specific Gravity, and Bulk Density of Refractory Shapes by Vacuum Pressure.
42. Principles of Ceramic Processing, James Reed Chapter 26, John Wiley & Sons, 1974